Coulomb Blockade in a Nonthermalized Quantum Dot

G. McArdle,[1] R. Davies,[2] I. V. Lerner,[1,*] and I. V. Yurkevich[2]
[1]School of Physics and Astronomy, University of Birmingham, Birmingham, B15 2TT, United Kingdom
[2]School of Computer Science and Digital Technologies, Aston University, Birmingham, B4 7ET, United Kingdom

(Received 6 June 2023; accepted 12 October 2023; published 15 November 2023)

We investigate nonequilibrium transport properties of a quantum dot in the Coulomb blockade regime under the condition of negligible inelastic scattering during the dwelling time of the electrons in the dot. Using the quantum kinetic equation we show that the absence of thermalization leads to a double step in the distribution function of electrons on the dot, provided that it is symmetrically coupled to the leads. This drastically changes nonlinear transport through the dot resulting in an additional (compared to the thermalized case) jump in the conductance at voltages close to the charging energy, which could serve as an experimental manifestation of the absence of thermalization.

DOI: 10.1103/PhysRevLett.131.206303

Many-body localization (MBL), predicted for disordered many-electron systems which are not thermalized with the environment [1,2], has attracted a lot of theoretical and experimental attention (for a review, see [3]) and has been observed in systems of ultracold atoms [4]. One of the defining properties of MBL is the absence of thermalization [5,6].

Prior to the MBL papers [1,2], a similar regime of localization in Fock space was predicted for quantum dots [7] where electrons fail to mutually equilibrate as their dwelling time on the dot, τ_{dw}, is much shorter than the equilibration time τ_{eq}. Alternatively, this condition can be formulated as

$$\gamma \ll \Gamma, \tag{1}$$

where $\gamma \sim 1/\tau_{\mathrm{eq}}$ is the equilibration rate and $\Gamma \sim 1/\tau_{\mathrm{dw}}$ is the tunneling rate. For a zero-dimensional diffusive dot, the electron-electron equilibration rate [7–9],

$$\gamma \approx \Delta\left(\frac{\varepsilon}{g\Delta}\right)^2, \tag{2}$$

can be sufficiently small provided that $\sqrt{g}\Delta < \varepsilon < g\Delta$, where ε is the quasiparticle energy, Δ is the mean level spacing on the dot, and $g\Delta$ is the Thouless energy of the dot with dimensionless conductance $g \gg 1$.

In this Letter, we show that such an absence of thermalization leads to striking changes in nonlinear transport in the Coulomb blockade regime, where electrons are loaded one by one into a quantum dot due to the charging energy, $E_{\mathrm{c}} = e^2/C$, of a dot of capacitance C, preventing a continuous flow. We assume the separation of scales typical for the classical Coulomb blockade at a temperature T (see [10–12] for reviews):

$$\Gamma \ll \Delta \ll T \ll E_{\mathrm{c}}. \tag{3}$$

Typically, the study of quantum dots in the Coulomb blockade regime has been focused on the regime where complete thermalization is assumed. This regime is characterized by peaks in the conductance as a function of gate voltage [13,14] that can be attributed to interesting features in the tunneling density of states [15], and—in case of strong asymmetry in the coupling to the leads—by a staircase in the current as a function of the bias voltage V [16–19]. When the coupling is approximately symmetric, $\Gamma_{\mathrm{L}} \sim \Gamma_{\mathrm{R}}$, the Coulomb staircase practically vanishes in the thermalized case. But it is precisely in this case when the absence of thermalization reveals itself by an additional jump in the nonlinear differential conductance, as we show in this Letter by solving the quantum kinetic equation. The absence of thermalization on a dot, therefore, can be detected by this jump which occurs within the first step of the Coulomb staircase.

The jump arises due to the change in the distribution function of the dot; going from a Fermi function in the fully thermalized case to a double-step form. A similar structure (although for practically noninteracting electrons) has previously been observed in one-dimensional wires where the distribution function was a linear combination of the two Fermi functions of the leads due to insufficient time for equilibration [20]. A double-step distribution has also been predicted for open quantum dots, where electrons are practically noninteracting [21], and for auxiliary noninteracting

electrons in the slave-boson approach to the Kondo effect in quantum dots [22]. Here, in the Coulomb-blockade regime in region (3), a double-step form of the electron distribution function is substantially modified by the interaction.

The standard Hamiltonian of a Coulomb-blockaded quantum dot coupled to two leads is $H = H_{\rm dot} + H_{\rm l} + H_{\rm tun}$, where

$$H_{\rm dot} = \sum_n \varepsilon_n d_n^\dagger d_n + \frac{1}{2} E_{\rm c} (\hat{N} - N_{\rm g})^2, \tag{4a}$$

$$H_{\rm l} = \sum_{k,\alpha} (\varepsilon_k - \mu_\alpha) c_{k,\alpha}^\dagger c_{k,\alpha}, \tag{4b}$$

$$H_{\rm tun} = \sum_{k,n,\alpha} (t_\alpha c_{k,\alpha}^\dagger d_n + {\rm H.c.}). \tag{4c}$$

Here, $\alpha = {\rm L}, {\rm R}$ labels the leads, $d_n^\dagger(d_n)$, $c_{k,\alpha}^\dagger(c_{k,\alpha})$ are the creation (annihilation) operators for electrons with energies ε_n and ε_k in the dot and leads, respectively, $\hat{N} = \sum_n d_n^\dagger d_n$ is the number operator for the dot, and $N_{\rm g}$ is the preferred number of electrons on the dot set by the gate voltage. The leads have chemical potentials $\mu_{\rm L} = \mu + eV$ and $\mu_{\rm R} = \mu$. The k- and n-independent tunneling amplitudes between the dot and leads, t_α, define, along with the density of states of the leads ν_α (taken to be constant), the tunneling rates $\Gamma_\alpha = 2\pi\nu_\alpha |t_\alpha|^2$ with the total $\Gamma = \Gamma_{\rm L} + \Gamma_{\rm R}$.

In addition to inequalities (3), we assume that the Fermi energy of the dot is much larger than the charging energy, $\varepsilon_{\rm F} \gg E_{\rm c}$, to ensure that only electrons in a relatively narrow energy strip around $\varepsilon_{\rm F}$ contribute the transport properties of the system. This assumption is also utilized in the orthodox theory of the Coulomb blockade [14,16–19] and is achievable in experiments [10,23]. By starting with the standard expression for tunneling current [24] and assuming current conservation, we express the current across a quantum dot in the Coulomb blockade regime in the region (3) as

$$I = e\frac{\Gamma_{\rm L}\Gamma_{\rm R}}{\Gamma} \sum_{N,n} p_N \big(F_N(\varepsilon_n)[f_{\rm L}(\varepsilon_n + \Omega_{N-1}) - f_{\rm R}(\varepsilon_n + \Omega_{N-1})] + [1 - F_N(\varepsilon_n)][f_{\rm L}(\varepsilon_n + \Omega_N) - f_{\rm R}(\varepsilon_n + \Omega_N)] \big), \tag{5}$$

with details of the derivation in Supplemental Material [25]. Here, p_N is the probability of N electrons being on the dot, $F_N(\varepsilon_n)$ is their distribution function, and $f_{\rm L,R}(\varepsilon_n)$ are Fermi functions in the leads with chemical potentials $\mu_{\rm L} = \mu + eV$ and $\mu_{\rm R} = \mu = \varepsilon_{\rm F}$ respectively. The presence of the charging energy is encapsulated by

$$\Omega_N = E_{N+1} - E_N = E_{\rm c}\left(N + \frac{1}{2} - N_{\rm g}\right), \tag{6}$$

where $E_N = \frac{1}{2} E_{\rm c}(N - N_{\rm g})^2$.

The current through a thermalized quantum dot is usually considered with the help of a master equation [13,14,16–19] involving electrons of all energies. In the nonthermalized regime (1), the electrons with different energies are not mixed. Hence, the probabilities and distribution functions can be found from the energy-conserving quantum kinetic equation (QKE), which is formulated using the Keldysh formalism (see, e.g., [24,26,27]) in terms of the "greater," $g^>(t)$, and "lesser," $g^<(t)$, Green's function of the dot. In the regime (3), where the mean level spacing is much larger than the level broadening due to tunneling, they are split into a sum over the energy levels, with Green's function for the nth level given by $g_n^>(t) = -i\langle d_n(t) d_n^\dagger(0)\rangle$ and $g_n^<(t) = i\langle d_n^\dagger(0) d_n(t)\rangle$, where $d_n(t) = {\rm e}^{iHt} d_n {\rm e}^{-iHt}$. Then, to linear order in tunneling, the QKE is reduced to [24,26,27],

$$g_n^>(\varepsilon)\Sigma^<(\varepsilon) = g_n^<(\varepsilon)\Sigma^>(\varepsilon). \tag{7}$$

Here, the conservation of particle number for an isolated dot allows one to represent the single-level Green's functions as (see Supplemental Material [25])

$$g_n^>(\varepsilon) = -2\pi i \sum_N \delta(\varepsilon - \varepsilon_n - \Omega_N) p_N [1 - F_N(\varepsilon_n)],$$
$$g_n^<(\varepsilon) = 2\pi i \sum_N \delta(\varepsilon - \varepsilon_n - \Omega_{N-1}) p_N F_N(\varepsilon_n), \tag{8}$$

with the normalization $\sum_N p_N = 1$. The self-energy functions of the leads in Eq. (7) are assumed to be n independent and are given by

$$\Sigma^>(\varepsilon) = i \sum_{\alpha={\rm L,R}} \Gamma_\alpha [f_\alpha(\varepsilon) - 1], \qquad \Sigma^<(\varepsilon) = i \sum_{\alpha={\rm L,R}} \Gamma_\alpha f_\alpha(\varepsilon). \tag{9}$$

Substituting Eqs. (8) and (9) into Eq. (7) leads to the QKE reflecting the detailed balance equations, coinciding with those derived in [14] for $\Delta \gg T$,

$$p_{N+1} F_{N+1}(\varepsilon_n)[1 - \tilde{f}(\varepsilon_n + \Omega_N)] = p_N [1 - F_N(\varepsilon_n)] \tilde{f}(\varepsilon_n + \Omega_N),$$
$$\tilde{f}(\varepsilon) = (\Gamma_{\rm L}/\Gamma) f_{\rm L}(\varepsilon) + (\Gamma_{\rm R}/\Gamma) f_{\rm R}(\varepsilon). \tag{10}$$

It is this equation along with the normalization conditions, $\sum_N p_N = 1$ and $\sum_n F_N(\varepsilon_n) = N$, that can be used to obtain the probabilities and distribution functions required in

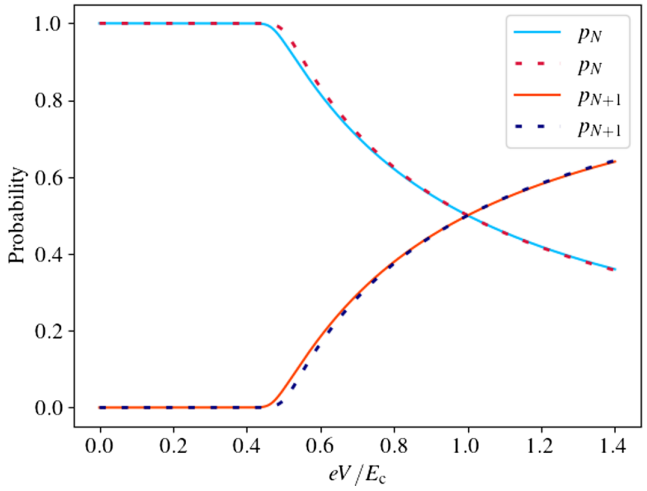

FIG. 1. The occupation probabilities p_N (the upper line) and p_{N+1} (the lower line) as functions of bias voltage, V, for $\Gamma_L = \Gamma_R$, and $N = N_g$. Here, they depend only on the ratio E_c/T in the temperature region 10–100 mK, albeit this dependence is rather weak ($E_c/T = 100$ was used for this figure). The solid lines represent our results for the nonthermalized case, the dashed lines for the full-thermalization case [16–19]. In this temperature range they are practically indistinguishable.

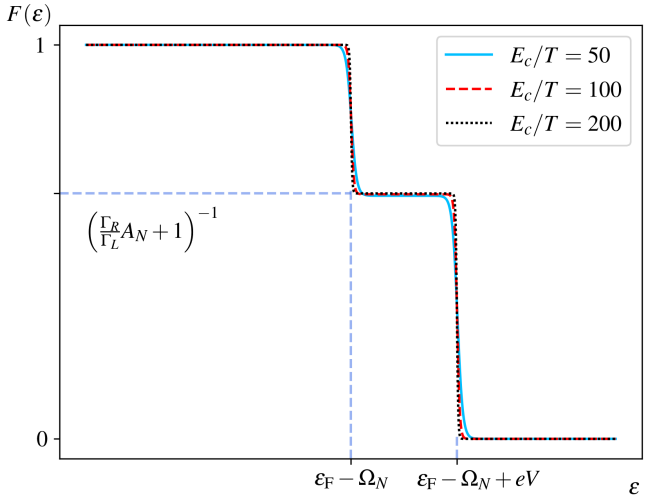

FIG. 2. The electron distribution function in the dot for $\Gamma_L = \Gamma_R$, $N = N_g$, and $eV = 0.8E_c$ where $A_N \approx 0.6$ (as found numerically). The double-step structure is robust as long as $eV > \Omega_N$—in the opposite case $A_N \equiv p_{N+1}/p_N \to 0$, as seen from Fig. 1, and the middle step disappears. $F(\varepsilon)$ has only a weak dependence on E_c/T so that the three curves above practically merge.

Eq. (5) to calculate the current. The results for full thermalization are recovered by summing Eq. (10) over n using the fact that in this case we can substitute the equilibrium distribution function, $F_N(\varepsilon_n) = f(\varepsilon_n - \varepsilon_F)$.

The absence of thermalization, however, drastically changes the distribution function. In this case, QKE (10) has an exact solution providing there are only two relevant states (N and $N+1$) for a given voltage (see Supplemental Material [25]). In the case of approximately equal coupling, this condition can be satisfied only for a finite bias window, i.e., within the first step of the Coulomb staircase. For higher bias, one needs to account for more states with different numbers of particles that are not being exponentially suppressed (in contrast to the asymmetric case when $\Gamma_L/\Gamma_R \gg 1$ [28]).

Assuming that the chemical potential in the dot is of order of the unbiased chemical potential in the (right) lead, we show that the current and, hence, the differential conductance has an additional peak in the window $0 \leq eV \lesssim \Omega_{N+1}$ as compared to the thermalized case [16–19]. In this window, where only two levels are relevant, the kinetic equation (10) has the solution $F_N(\varepsilon_n) \approx F_{N+1}(\varepsilon_n) \approx F(\varepsilon_n)$ in the limit $N \gg 1$, leading to

$$F(\varepsilon_n) = \frac{\tilde{f}(\varepsilon_n + \Omega_N)}{[1 - \tilde{f}(\varepsilon_n + \Omega_N)]A_N + \tilde{f}(\varepsilon_n + \Omega_N)}, \qquad (11)$$

where $A_N = p_{N+1}/p_N$. This ratio of probabilities is found from normalization, $N = \sum_n F(\varepsilon_n) = (1/\Delta)\int_0^\infty F(\varepsilon)\mathrm{d}\varepsilon$, while $p_N + p_{N+1} = 1$ as shown in Supplemental Material [25]. As seen in Fig. 1, depicted for the middle of the Coulomb blockade valley where $\Omega_N = E_c/2$, both p_N and p_{N+1} are practically indistinguishable from the thermalized case. It remains the case as long as Ω_N, Eq. (6), remains far from the peaks of the Coulomb blockade. Note that this and all subsequent results depend only on ratios of energetic parameters and are fully applicable in experimental regimes where $T \sim 10$–100 mK and $E_c \sim 1$ meV.

On the contrary, the distribution function, found by substituting the ratio $A_N \equiv p_{N+1}/p_N$ into Eq. (11), acquires an additional step

$$F(\varepsilon_n) \approx \begin{cases} 1, & \varepsilon_n < \mu_R - \Omega_N \\ \left(1 + \frac{\Gamma_R}{\Gamma_L}A_N\right)^{-1}, & \mu_R - \Omega_N < \varepsilon_n < \mu_L - \Omega_N \\ 0. & \mu_L - \Omega_N < \varepsilon_n \end{cases} \qquad (12)$$

as depicted for the middle of the valley in Fig. 2. Such a double step is similar to that observed in short quasi-one-dimensional wires [20]. However, in the wire the double step was simply a linear combination of the two Fermi functions of the leads, while in the present case it is substantially affected by the Coulomb interaction. Still, in both cases the double step reflects the lack of thermalization between electrons coming from the left and right leads. In the steady-state limit, electrons from both leads enter the dot at two different chemical potentials and thermalize with the opposite lead only after exiting the dot. Note that the double step is effectively washed out in the one-lead limit of the Coulomb blockade when $\Gamma_R/\Gamma_L \ll 1$.

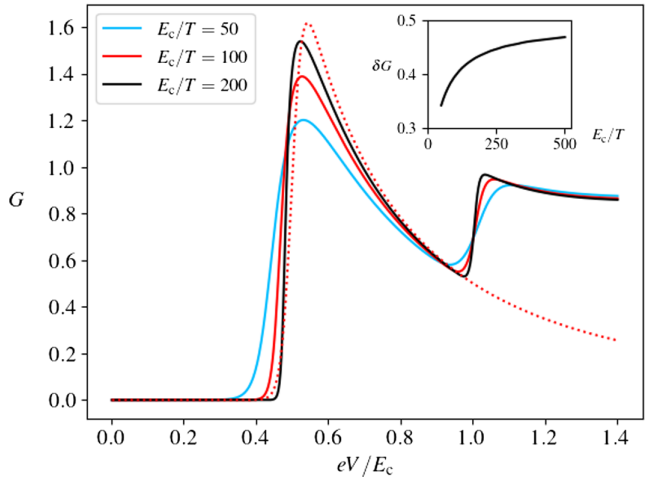

FIG. 3. The differential conductance, $G(V)$, in units of $(e^2/\Delta)(\Gamma_L\Gamma_R/\Gamma) \approx (e^2\Gamma/4\Delta)$ when $\Gamma_L \approx \Gamma_R$. For $\Gamma_L \sim \Gamma_R$, an additional jump in G is always at $eV = E_c$. Such a jump is absent in the thermalized case [16–19], depicted here by the dotted line for $E_c/T = 100$. The dependence of its height, δG, on the ratio E_c/T, is shown in the inset.

The double-step distribution in the dot drastically changes the differential conductance, $G = dI/dV$, in comparison with the thermalized case [16–19]. Substituting p_N and $F(\varepsilon_n)$ into Eq. (5) with $F_N(\varepsilon_n) \approx F(\varepsilon_n)$, we find G as shown in Fig. 3. For small voltages, $eV < E_c$, the absence of thermalization has little impact in the low-T limit. However, at $eV = E_c$, there appears a secondary jump in the nonthermalized case. It is robust as long as the tunneling is symmetric, $\Gamma_L \approx \Gamma_R$, when there are three distinct regions for the distribution, Eq. (12). Rewriting Eq. (5) for the current in the low-T limit and for $eV \lesssim \Omega_{N+1}$ will make this clearer:

$$I = \frac{e}{\Delta}\frac{\Gamma_L\Gamma_R}{\Gamma}\left(p_N\int_{\mu-\Omega_{N-1}}^{\mu-\Omega_{N-1}+eV} F(\varepsilon)d\varepsilon + \int_{\mu-\Omega_N}^{\mu-\Omega_N+eV}\{p_N[1-F(\varepsilon)] + p_{N+1}F(\varepsilon)\}d\varepsilon + p_{N+1}\int_{\mu-\Omega_{N+1}}^{\mu-\Omega_{N+1}+eV}[1-F(\varepsilon)]d\varepsilon\right). \quad (13)$$

The second integration over the middle step starts to contribute at $eV \gtrsim E_c/2$ when p_N and p_{N+1} start to change, see Fig. 1, signaling that the oncoming particle is sufficiently energetic to overcome the charging energy. This results in the usual blockade jump which is the same for both the thermalized and nonthermalized cases. As long as $eV < E_c$, the first and third integrals in Eq. (13) are negligible as the each integration is over a region where the integrands are exponentially small at $T \ll E_c$. For $eV \gtrsim E_c$, this is no longer the case and the appropriate nonzero contribution results in a sudden change in the current revealed as a jump in the differential conductance at $eV = E_c$.

The position of this jump is insensitive to gate voltage as it only depends on the difference $\Omega_{N+1} - \Omega_N = E_c$. In the region around the jump, the ratio of probabilities is given for $T \ll E_c$ (see Supplemental Material [25]) by

$$A_N \equiv \frac{p_{N+1}}{p_N} \approx \frac{\Gamma_L}{\Gamma_R}\left(\frac{eV-\Omega_N}{\Omega_N}\right). \quad (14)$$

Then, calculating the current from Eq. (13) on both sides of the jump we find that the jump in the differential conductance, neglecting corrections in T/E_c, has the height

$$\delta G = \frac{e^2}{2\Delta}\frac{\Gamma_L\Gamma_R}{\Gamma}, \quad (15)$$

in the middle of the Coulomb blockade valley, $\Omega_N = \frac{1}{2}E_c$. (The general expression for δG is given in Supplemental Material [25]). This jump is rather robust: it occurs at $eV = E_c$ independently of Ω_N and has only a weak temperature dependence. As the temperature is increased, while still obeying inequalities (3), the jump is only slightly smeared across a wider range of voltages as shown in the inset in Fig. 3. This jump should be experimentally observable and give a clear indication of the absence of thermalization within a quantum dot.

In conclusion, we note that the existence of additional fine structure of the Coulomb blockade peaks has been established numerically and experimentally [29] for small dots, where $\Delta \gg T$. Here, we have considered the opposite case of large quantum dots (3), where we have shown that the absence of thermalization manifests itself as an additional jump in the differential conductance at $eV = E_c$, which follows the usual jump at $eV = \Omega_N$. This is a direct consequence of the lack of equilibration between electrons coming from the left and right leads so that the distribution function on the dot has a double-step form. We anticipate this jump to be experimentally accessible at the appropriate voltages and therefore could be used as a method of identifying the absence of thermalization in the dot.

We gratefully acknowledge support from EPSRC under Grant No. EP/R029075/1 (I. V. L.) and from the Leverhulme Trust under Grant No. RPG-2019-317 (I. V. Y.).

*Corresponding author: i.v.lerner@bham.ac.uk

[1] D. Basko, I. Aleiner, and B. Altshuler, Metal-insulator transition in a weakly interacting many-electron system with localized single-particle states, Ann. Phys. (Amsterdam) **321**, 1126 (2006).

[2] I. V. Gornyi, A. D. Mirlin, and D. G. Polyakov, Interacting electrons in disordered wires: Anderson localization and low-t transport, Phys. Rev. Lett. **95**, 206603 (2005).

[3] D. A. Abanin and Z. Papić, Recent progress in many-body localization, Ann. Phys. (Amsterdam) **529**, 1700169 (2017).
[4] M. Schreiber, S. S. Hodgman, P. Bordia, H. P. Lüschen, M. H. Fischer, R. Vosk, E. Altman, U. Schneider, and I. Bloch, Observation of many-body localization of interacting fermions in a quasirandom optical lattice, Science **349**, 842 (2015).
[5] R. Nandkishore and D. A. Huse, Many-body localization and thermalization in quantum statistical mechanics, Annu. Rev. Condens. Matter Phys. **6**, 15 (2015).
[6] M. Serbyn, D. A. Abanin, and Z. Papić, Quantum many-body scars and weak breaking of ergodicity, Nat. Phys. **17**, 675 (2021).
[7] B. L. Altshuler, Y. Gefen, A. Kamenev, and L. S. Levitov, Quasiparticle lifetime in a finite system: A nonperturbative approach, Phys. Rev. Lett. **78**, 2803 (1997).
[8] U. Sivan, Y. Imry, and A. G. Aronov, Quasi-particle lifetime in a quantum dot, Europhys. Lett. **28**, 115 (1994).
[9] Y. M. Blanter, Electron-electron scattering rate in disordered mesoscopic systems, Phys. Rev. B **54**, 12807 (1996).
[10] L. P. Kouwenhoven, C. M. Marcus, P. L. McEuen, S. Tarucha, R. M. Westervelt, and N. S. Wingreen, Electron transport in quantum dots, in *Mesoscopic Electron Transport*, edited by L. L. Sohn, L. P. Kouwenhoven, and G. Schön (Springer Netherlands, Dordrecht, 1997), pp. 105–214.
[11] I. L. Aleiner, P. W. Brouwer, and L. I. Glazman, Quantum effects in Coulomb blockade, Phys. Rep. **358**, 309 (2002).
[12] Y. Alhassid, The statistical theory of quantum dots, Rev. Mod. Phys. **72**, 895 (2000).
[13] D. V. Averin and K. K. Likharev, Coulomb blockade of single-electron tunneling, and coherent oscillations in small tunnel junctions, J. Low Temp. Phys. **62**, 345 (1986).
[14] C. W. J. Beenakker, Theory of Coulomb-blockade oscillations in the conductance of a quantum dot, Phys. Rev. B **44**, 1646 (1991).
[15] N. Sedlmayr, I. V. Yurkevich, and I. V. Lerner, Tunnelling density of states at Coulomb-blockade peaks, Europhys. Lett. **76**, 109 (2006).
[16] I. O. Kulik and R. I. Shekhter, Kinetic phenomena and charge discreteness effects in granulated media, Zh. Eksp. Teor. Fiz. **68**, 623 (1975), http://jetp.ras.ru/cgi-bin/dn/e_041_02_0308.pdf.
[17] D. Averin and K. Likharev, A correlated transfer of single electrons and Cooper pairs in systems of small tunnel junctions, in *Mesoscopic Phenomena in Solids*, Modern Problems in Condensed Matter Sciences Vol. 30, edited by B. Altshuler, P. Lee, and R. Webb (Elsevier, Amsterdam, 1991), pp. 173–271.
[18] M. Amman, R. Wilkins, E. Ben-Jacob, P. D. Maker, and R. C. Jaklevic, Analytic solution for the current-voltage characteristic of two mesoscopic tunnel junctions coupled in series, Phys. Rev. B **43**, 1146 (1991).
[19] D. V. Averin, A. N. Korotkov, and K. K. Likharev, Theory of single-electron charging of quantum wells and dots, Phys. Rev. B **44**, 6199 (1991).
[20] H. Pothier, S. Guéron, N. O. Birge, D. Esteve, and M. H. Devoret, Energy distribution function of quasiparticles in mesoscopic wires, Phys. Rev. Lett. **79**, 3490 (1997).
[21] A. Altland and R. Egger, Nonequilibrium dephasing in Coulomb blockaded quantum dots, Phys. Rev. Lett. **102**, 026805 (2009).
[22] S. Smirnov and M. Grifoni, Slave-boson Keldysh field theory for the Kondo effect in quantum dots, Phys. Rev. B **84**, 125303 (2011).
[23] L. P. Kouwenhoven, N. C. van der Vaart, A. T. Johnson, W. Kool, C. J. P. M. Harmans, J. G. Williamson, A. A. M. Staring, and C. T. Foxon, Single electron charging effects in semiconductor quantum dots, Z. Phys. B **85**, 367 (1991).
[24] A.-P. Jauho, N. S. Wingreen, and Y. Meir, Time-dependent transport in interacting and noninteracting resonant-tunneling systems, Phys. Rev. B **50**, 5528 (1994).
[25] See Supplemental Material at http://link.aps.org/supplemental/10.1103/PhysRevLett.131.206303 for additional details on (i) deriving the Green's functions and current formula, (ii) solving the QKE, and (iii) obtaining the probabilities and height of the additional jump.
[26] J. Rammer and H. Smith, Quantum field-theoretical methods in transport theory of metals, Rev. Mod. Phys. **58**, 323 (1986).
[27] H. Haug and A.-P. Jauho, *Quantum Kinetics in Transport and Optics of Semiconductors* (Springer, Berlin, 1998).
[28] G. McArdle, R. Davies, I. V. Lerner, and I. V. Yurkevich, Coulomb staircase in an asymmetrically coupled quantum dot, J. Phys. Condens. Matter **35**, 475302 (2023).
[29] O. Agam, N. S. Wingreen, B. L. Altshuler, D. C. Ralph, and M. Tinkham, Chaos, interactions, and nonequilibrium effects in the tunneling resonance spectra of ultrasmall metallic particles, Phys. Rev. Lett. **78**, 1956 (1997).